JOURNAL OF GUIDANCE, CONTROL, AND DYNAMICS
Vol. 30, No. 1, January–February 2007

Design and Evaluation of a Haptic Flight Director

S. de Stigter,* M. Mulder,† and M. M. van Paassen‡
Delft University of Technology, 2629 HS Delft, The Netherlands

DOI: 10.2514/1.20593

The majority of information sources on the flight deck are visual displays. An example is the flight director display that improves pilot manual aircraft control performance but also involves a visually demanding task. Tactile, or *haptic* displays use the human tactile modality as an information channel. This paper discusses how the visual information of the flight director can be presented through providing force-feedback on the control stick. The haptic flight director gives pilots a constant stream of tactile information on the state of the flight director command bars, also when visual attention is not directed at the primary flight display. It was hypothesized that the shorter latencies in the tactile motor loop allow pilots to control aircraft at a higher bandwidth, increasing performance. It was further hypothesized that using two modalities, instead of one, to conduct the aircraft manual control task, would reduce pilot workload, also when a secondary, visually distracting side task is present. To test these hypotheses, an experiment was conducted in a fixed-base simulator. Professional pilots conducted approaches with the visual and haptic flight director displays, while simultaneously a secondary task had to be conducted. Results show that the haptic flight director indeed yields improved pilot performance and lower workload.

Nomenclature

M_x, M_y	=	stick roll, pitch moment, N · m
T_{int}	=	secondary task interval time, s
T_p	=	prediction time, s
T_{task}	=	secondary task execution time, s
χ_e	=	aircraft track angle error, deg
x_e, z_e	=	aircraft lateral, vertical position error, m
γ_e	=	aircraft flight-path angle error, deg
δ_a, δ_e	=	aileron, elevator control angle, deg
$\dot{\delta}_a$, $\dot{\delta}_e$	=	aileron, elevator control rate, deg /s
θ_x, θ_y	=	stick roll, pitch position, deg
ϕ, θ	=	aircraft roll, pitch attitude, deg
$\dot{\phi}$, $\dot{\theta}$	=	aircraft roll rate, pitch rate, deg /s

I. Introduction

SITUATION awareness results from the continuous visual sampling and monitoring of the cockpit instruments. Generally speaking, a pilot scans the cockpit instruments and forms a mental model of the statistical properties of events that these instruments display. Research shows that human visual sampling is not optimal, however, and suffers from complications like fixation and oversampling when sampling multiple sources is required [1–3].

An example of a visual display that requires continuous scanning is the flight director display. Flight directors were introduced to simplify the pilot manual control task through display augmentation. Two command bars presented on the primary flight display indicate the required control actions to conduct a particular task, defined by the pilot, reducing aircraft manual control to a compensatory tracking task. A disadvantage of the flight director is that it requires much of the pilot's visual attention, and when the pilot is distracted and has to put attention elsewhere, performance deteriorates considerably [4–6].

Multiple resource theory states that dividing attention between modalities can be more efficient, effectively lowering the workload involved in scanning as compared with dividing attention within a single modality [7]. Hence, a better division of the flight deck information sources over different modalities might allow pilots to reduce their scanning effort, while maintaining or even improving performance. In present cockpits, nonvisual information sources such as auditory signals are generally used to direct pilot's attention to the visual displays. The use of the tactile modality is limited (e.g., trim forces) or only present to inform pilots of non-nominal flight conditions (e.g., stick shaker).

In this paper it will be described how the motion of the flight director command bars can be presented to pilots through providing tactile information on the control stick, in addition to the visual presentation. It was hypothesized that this so-called haptic flight director display may result in two advantages. First, previous research showed that shorter latencies in the tactile-motor control loop yield an increased manual control performance [8,9]. The equivalence in what the pilot sees on the visual display and what is felt in the control stick may result in cooperation or even integration of the two information channels [10]. Second, the haptic flight director display provides pilots with continuous tactile information on the primary control task. This could allow pilots to temporarily discard the visual flight director display when an event presented on another visual display requires their attention.

The objective of this paper is to explore the potential benefits of the haptic flight director, in terms of pilot manual control performance, workload, and the efficiency in sharing attention. It is structured as follows. The first theoretical part describes how the haptic flight director display was designed, and discusses how the control laws were tuned. In the second part the results of an experiment will be described, in which professional airline pilots conducted manual approaches using the visual and haptic flight director displays.

II. Design of the Haptic Flight Director

A. Visual and Haptic Display Augmentation

1. The Conventional, Visual Flight Director

In manual aircraft control, pilots determine the proper control actions through sampling and mentally integrating various displays on the flight deck. To increase pilot performance and reduce workload the flight director (FD) has been developed, a control system that automatically integrates the aircraft states into two

Received 17 October 2005; revision received 4 April 2006; accepted for publication 5 April 2006.

*Research Associate, Control and Simulation Division, Faculty of Aerospace Engineering, Kluyverweg 1; sebastiaan@destigter-photography.com

†Associate Professor, Control and Simulation Division, Faculty of Aerospace Engineering, Kluyverweg 1; m.mulder@tudelft.nl. Member AIAA.

‡Associate Professor, Control and Simulation Division, Faculty of Aerospace Engineering, Kluyverweg 1; m.m.vanpaassen@tudelft.nl. Member AIAA.

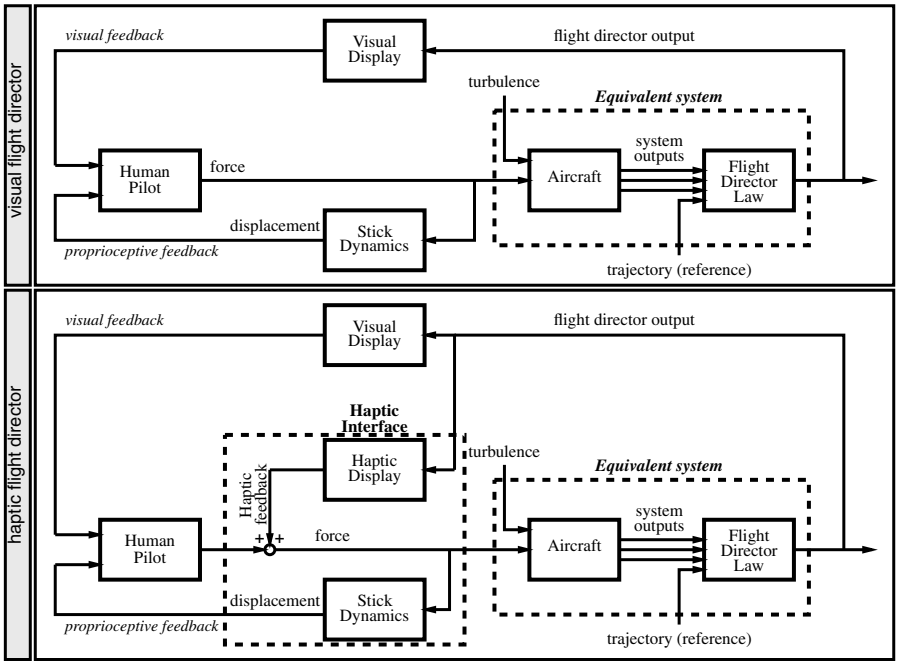

Fig. 1 Visual and haptic flight directors.

steering commands. These are presented as two moving flight director command bars on the primary flight display, and represent the control actions required by the pilot to properly control the aircraft in a particular setting. With a flight director, the aircraft manual control task reduces to a compensatory tracking task.

The flight director is an example of display augmentation, and transforms the pilot manual control task from a computational task to a merely perceptual task, with simplified dynamics. Figure 1 (top) shows a schematic of the display augmentation principle using the visual flight director. The flight director changes the equivalent dynamics of the manual control task, because the pilot is now controlling the combination of the aircraft dynamics and the dynamics introduced by the flight director control laws. When done properly, these control laws cancel out part of the aircraft dynamics, significantly reducing the order of control, preferably to a single integrator over a wide frequency range [11]. This allows pilots to act as a simple, proportional controller near the crossover frequency, a control strategy that is highly preferred [12].

The use of the (visual) flight director display augmentation can be best explained using an example involving only lateral (or roll) control, illustrated in Fig. 2 (top-left and bottom-left). The aircraft is assumed to be located to the left of the reference trajectory. The vertical flight director command bar indicates that the pilot needs to control the aircraft to roll right, i.e., the stick must be moved from its middle position to the right. The vertical bar will then move back to the center of the display. As the pilot control stick deflection is proportional to the indicated flight director error, e_{FD}, it is gradually reduced until both the FD command bar and the stick are centered. In terms of forces on the stick, with a common spring-loaded stick the pilot first experiences a large force as he or she moves the stick to the right, and consequently, when the flight director command bar moves back to the center, the force applied to the stick decreases. The process of building up and reducing the force on the stick can be regarded as a washing-out effect. For most readers, this explanation is trivial, but it will be of use when explaining the more complicated haptic flight director, discussed next.

2. *A Tactile, Haptic Flight Director*

The conventional flight director provides two-dimensional, pitch and roll, display augmentation on a compensatory visual display. In this paper a different approach is explored, namely, the presentation of the flight director command bars through providing a tactile

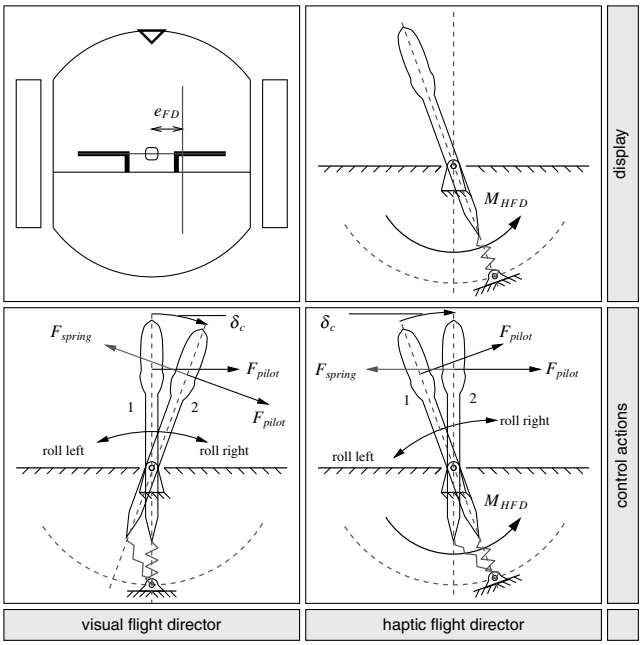

Fig. 2 The working principles of the visual (left) and haptic (right) flight directors.

feedback on the pilot's control stick. The resulting haptic flight director is expected to yield similar benefits in terms of simplifying the manual control task, yet more intuitive, closer to the source of control (i.e., the control stick), resulting in a larger bandwidth and therefore better performance. The concept of the haptic flight director (HFD) is illustrated in Fig. 1 (bottom).[§]

The design of the haptic display implies that the visual-motor task is converted into a tactile-motor task. The definition reflecting the flight director output and the corresponding tactile cues can be defined in a so-called haptic display law. The selection of this law must be done carefully as the tactile cues should provide the pilot

[§]In this work, the tactile information of the HFD is provided *in addition* to the visually displayed flight director command bars. The possibility of providing only haptic information is currently under investigation.

with information, while at the same time they should not interfere with the control task. Whereas control using the visual flight director makes use of two separate information channels, i.e., one for providing control direction (the movement of the flight director command bars) and one for receiving the pilot control inputs (the deflections of the control stick), the haptic flight director attempts to merge both into one channel, that is, the control stick. The selection of the haptic display law must satisfy the requirements to both communicate the flight director output, while at the same time it may not interfere with pilot control inputs, even when the pilot deliberately provides a control input that is opposite to what is commanded, for instance, in cases of emergency. Additionally, the use of the HFD should be both intuitive and, when feasible, resemble conventional manual control as close as possible. In that case, switching between manual control and control using the tactile feedback, and back, can occur naturally.

B. Design of the HFD

1. Force Tasks with Position Perturbations; Position Tasks with Force Perturbations

In tactile-motor studies, generally two different tasks are distinguished: 1) position tasks with force perturbations and 2) force tasks with position perturbations. In our context the "perturbations" are the tactile cues presented by the HFD, whereas the "task" represents what is asked of the pilot to control the aircraft.

In case of a force task with position perturbations, the stick dynamics must be uncompliant to the forces exerted on it to present the position perturbations, resulting in a control stick with infinite stiffness. The task is performed through exerting counteracting forces on the stick. Generally, it requires a very compliant behavior of the pilot, who must move along with the position perturbations of the uncompliant stick and controls the system by exerting forces on it.

In case of a position task with force perturbations, the compliant stick will be perturbed by external moments, while the task is performed by positioning of the stick, keeping it in the neutral position as good as possible. Here, a very tight grip to suppress the force perturbations is a likely control strategy. For prolonged periods, however, it may result in considerable physical fatigue [8].

Summarizing, whereas the force task with position perturbations would require an uncompliant stick, a situation that is highly unconventional for commercial aviation (some military aircraft form an exception to this), introducing the position task with force perturbations on the flight deck may result in undesirable pilot fatigue.

2. Force Task with Force Perturbations

Two other combinations of defining task and perturbations in haptic displays have not been discussed yet. Those are the position task with position perturbations and the force task with force perturbations. The first combination, however, makes no sense because any effort by the pilot is deemed useless, as the position of the uncompliant stick is unaffected by the external forces and, as such, no control inputs can be given.

The second combination, force tasks with force perturbations, is usually not applied because drifting of the stick may occur. However, when the control task is defined such that the force perturbations are applied on a stick with conventional mass-spring-damper dynamics, the force perturbations are equivalent to changing the stick equilibrium point. This is illustrated in Fig. 2 (right). Then, if the task is defined such that the correct, or desired, control actions are always directed to the center position of the stick, no drifting will occur. This configuration reduces the control task to mirroring the force perturbations that attempt to move the stick from its centered position. Mirroring these forces means that the pilot is indeed providing the desired control action, yielding the haptic equivalent of a visual flight director.

This approach results in a control stick that is compliant, like in conventional aircraft, allowing pilots to move the stick at will and overrule the tactile forces. It also allows for a reduced gain control, preventing fatigue because clamping the stick to its centered position is not necessary.

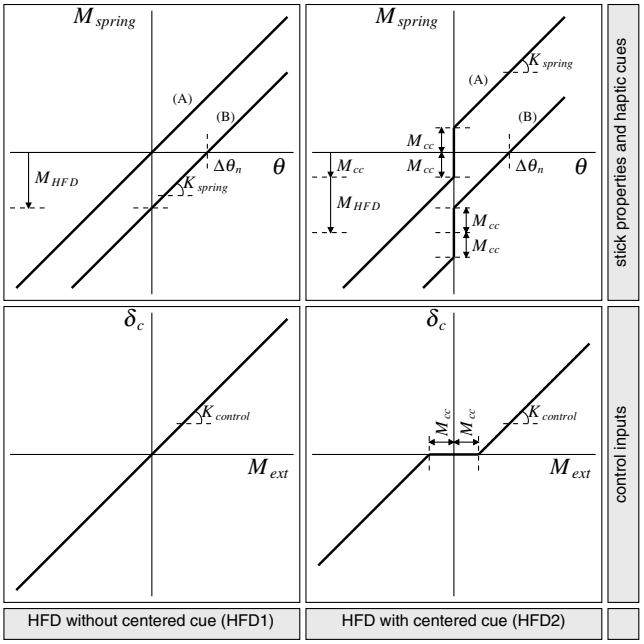

Fig. 3 Moment-position ($M_{\text{spring}} - \theta$, top) and moment-control command ($M_{\text{ext}} - \delta_c$, bottom) relations for HFD1 and HFD2.

3. Resemblance with the Visual Flight Director

In the force task with force perturbations, the motion of the flight director command bars is presented by a moment perturbation on the control stick, M_{HFD}. Figure 2 (top-right) illustrates that this moment essentially shifts the stick's neutral position, $\Delta\theta_n$ (see also Fig. 3, top-left), and is sensed by the pilot as a force perturbation on the hand. As soon as the pilot senses the stick moving from its centered position he or she simply exerts a small force in opposite direction, F_{pilot}, to reposition the stick, resulting in a spring reaction force F_{spring}. The exerted force by the pilot is then translated into a control command δ_c (Fig. 2, bottom-right), resulting in the flight director command bar moving to the center, lowering the sensed force perturbation. Correctly compensating for the flight director bar motion will feel like an external force that quickly washes out, in a similar way as with the visual flight director discussed in the preceding section.

Let us consider the same example as discussed in Sec. II.A.1 for the visual flight director. In situation 1 the visual flight director command bar (Fig. 2, top-left) indicates that the pilot should provide a roll command to the right. The haptic flight director, (Fig. 2, top-right) communicates this command to the pilot through a moment on the stick. If the pilot would not hold the stick, this would result in a new off-center (to the left) neutral point of the stick (Fig. 2, top-right), and nothing else would happen. If the pilot would hold the stick (loosely) in the hand, and compensates for the off-centered stick, he or she would introduce a force to the right (Fig. 2, bottom-right). This force results in a control input δ_c to the aircraft that would make it roll to the right. And as a result, the flight director command bar will start moving back to the center of the display, reducing the haptic flight director external moment and the corresponding off-centered neutral position of the stick. This results in the pilot continuously requiring less force to move the stick to the middle, i.e., the force washes out. The situation is resolved when the flight director bar is centered, no tactile cue is presented, and the stick is centered. This is all analogous to the visual flight director. In both cases, the pilot will exert the same force, in magnitude and direction, to move the stick from situation 1 to 2 in Fig. 2. With the HFD, the force will always be directed towards the stick center position, because the stick neutral point is manipulated by external moments, i.e., the tactile cues.

Table 1 Stick forward dynamics and haptic flight director settings as used in the experiment (pitch and roll axes are equal)

Parameter	Definition	Control type		
		VFD	HFD1	HFD2
Settings of the stick forward dynamics				
K_{spring}	Angular stiffness, N · m/rad	4.0	4.0	4.0
J_s	Rotational inertia, kg · m^2	0.01	0.01	0.01
B_s	Angular damping, N · ms/rad	0.2828	0.2828	0.2828
M_{cc}	Breakout moment, N · m	n/a	n/a	0.04
Characteristics of the haptic feedback				
$K_{\text{HFD}} = \partial M_{\text{HFD}}/\partial x_{e,p}\vert_{\text{TRK}}^{\text{pred}}$	HFD cue magnitude, N · m	n/a	16.0	16.0
$K_{\text{control}} = \partial \delta_c/\partial M_{\text{ext}}$	Control sensitivity, rad/N · m	0.06	0.06	0.06
$\Delta\theta_{\text{max,HFD}}$	Max. HFD neutral position shift, deg	n/a	15	15

4. *Presenting a Stick-Centered Cue*

A potential problem may result when the pilot's subjective stick-centered position does not coincide with the real centered position. This will result in the pilot controlling the aircraft with a bias error, e.g., steady flight parallel to the desired trajectory. To counter this potential problem, a small breakout moment (M_{cc} in Fig. 3, right) can be introduced that results in an additional cue indicating the stick's true center position.

Figure 3 illustrates the working principle of the center cue. It shows the stick stiffness relation, the effect of the haptic cues, and the control input relation, for both the haptic flight director without centered cue (HFD1) and the one with the centered cue (HFD2). Situation A represents the case where the flight director command signal is zero, whereas B shows the case for a nonzero command signal and the resulting moment perturbation M_{HFD}. In case of conventional control using the visual flight director (VFD), i.e., without haptics, the stick stiffness relation and control input relation are equal to HFD1, except of course that the stick stiffness relation remains constant.

Now that it is clear that both the task as well as the control input relations are equal for the visual flight director and the two haptic flight director settings (HFD1 and HFD2), a remarkable conclusion regarding the analogy in the required control forces can be drawn. Although the visual flight director requires the pilot to apply control forces that are directed away from the stick-centered position, and the haptic flight directors require these forces to be directed towards the stick-centered position, both the direction and magnitude of these forces are equal. That is, although the task has changed and the flight director command bars are presented with a different modality, the required pilot control actions remain unchanged.

5. *Experimental Settings of the Haptic Flight Director*

Table 1 summarizes the stick forward dynamics (i.e., the mass-spring-damper system) as well as the characteristics of the haptic feedback, for the three control types (VFD, HFD1, HFD2) that will be investigated in the experiment introduced in the next section.

The stick stiffness properties and centered-cue breakout force have been selected in cooperation with a professional pilot. The damping, B_s, was selected such that the damping ratio of the stick would equal $\sqrt{2}/2$. Similarly, the settings of the haptic flight director display have also been heuristically determined in accordance with comments from several test pilots. These pilots did not take part in the experiment.

III. Flight Director Control Law

In the preceding section, it was discussed how the flight director command bars can be presented with a visual display and a haptic display. Here the flight director control law will be described, i.e., the algorithm that integrates the information about the aircraft state relative to a reference condition into a desired control input, the flight director command signal.

This study focuses primarily on accurately controlling the aircraft along a reference trajectory. The control law to drive the flight director command bars, is based on an algorithm commonly used to drive flight-path predictor symbology in perspective flight-path displays [11,13–15]. Using the predicted aircraft position errors, in lateral and longitudinal directions, and presenting these using the vertical and horizontal flight director command bars, respectively, proved to be analogous as, if not equivalent to, more common yet more complex flight director control laws [16].

In this section, the principle of the control law and the procedure of tuning it are discussed.

A. Circular Flight-Path Predictor Algorithm

Figure 4 shows a simplified view of the so-called circular flight-path predictor algorithm, originally developed by Grunwald in the early 1980s [13], and extended and improved by others in later applications [11,15]. The principle of the algorithm is quite simple. It assumes that throughout the prediction span T_p, the aircraft speed V and both the lateral and vertical aircraft accelerations remain constant, resulting in a future path that is circular in both the lateral and vertical aircraft directions of motion. When the reference trajectory is known, the future aircraft position errors relative to this reference track can be easily computed.

The predicted lateral cross-track error $x_{e,p}$ can be approximated with [15]:

$$x_{e,p} = (x_e - x_c) + \chi_e V T_p + \dot{\chi}\frac{1}{2}VT_p^2 + K_{\dot{\phi}}\dot{\phi} \tag{1}$$

In this equation, x_c represents the lateral change of the reference trajectory within the prediction interval T_p, x_e represents the current aircraft cross-track error, χ_e the track angle error, and $\dot{\chi}$ its yaw rate, depending on the lateral acceleration. The last term on the right, $K_{\dot{\phi}}\dot{\phi}$, with $\dot{\phi}$ the aircraft roll rate, is known as the roll-rate extension to the classic algorithm, as introduced by Sachs [15]. The predicted vertical position error can be computed similarly.

B. Tuning the Flight-Path Prediction Algorithm

The flight-path prediction algorithm was tuned using a linearized model of the Cessna Citation 500 (altitude 1000 m, velocity V_{TAS} 51.4 m/s, clean configuration), the aircraft that will also be used in the experimental evaluation discussed in the next section [16].

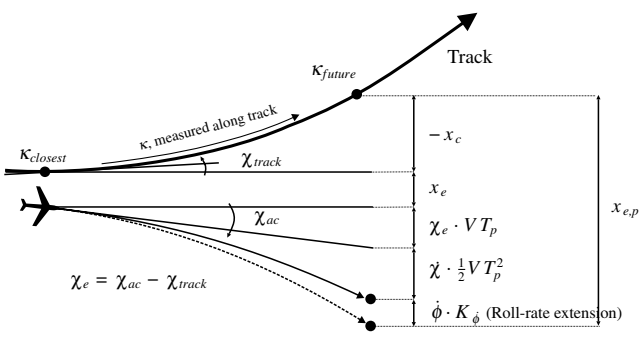

Fig. 4 Bird's eye view of the lateral flight-path predictor.

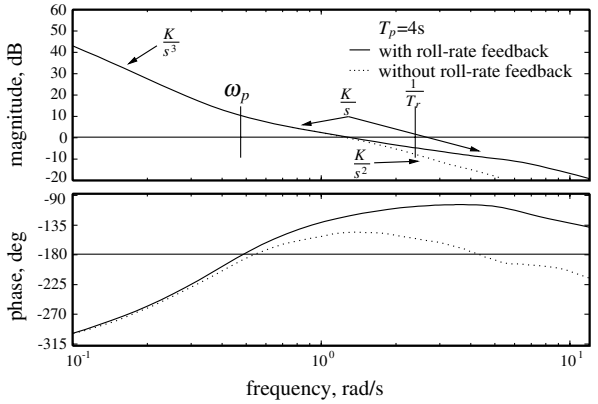

Fig. 5 Lateral open loop transfer function for predictor with/without roll-rate extension.

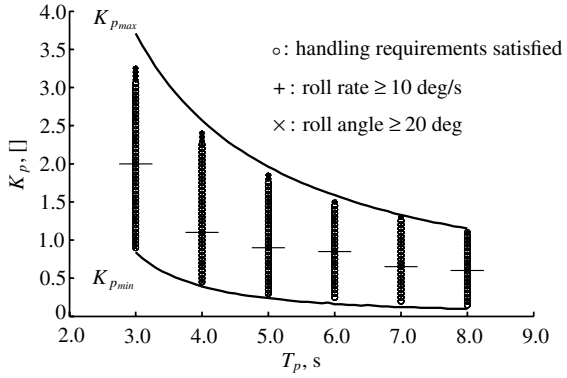

Fig. 6 Stability and handling pilot gain maxima and minima.

The principle of merging information about the aircraft state and the future reference trajectory, exemplified in Eq. (1), is quite similar to common flight director control laws. The dynamics introduced by this flight-path prediction algorithm effectively cancel a major part of the aircraft dynamics, reducing the order of control [11,15]. That is, when the pilot attempts to minimize the predicted lateral cross-track error $x_{e,p}$, he or she is controlling an equivalent system that is preferably an integrator over a wide range of frequencies.

Figure 5 shows that the equivalent dynamics of the aircraft + flight-path predictor combination are integratorlike over a wide range around the crossover frequency [11,15]. This allows the pilot to act as a proportional controller [12]:

$$H_{\text{pilot}} = \overbrace{K_p}^{\text{gain}} \overbrace{\left(\frac{-0.15s+1}{0.15s+1}\right)\left(\frac{1}{0.1s+1}\right)}^{\text{pilot limitations}} \tag{2}$$

with pilot gain K_p and including pilot limitations using a (Padé approximated) time delay of 0.3 s, and a neuromuscular lag of 0.1 s.

Using this pilot model and the linear Cessna Citation 500 aircraft model, 1512 flights were simulated along eight randomly-generated trajectories that consisted of straight legs and heading changes (3, 2.25, or 1.5 deg/s). The simulations were conducted for various combinations of prediction time T_p, ranging from 3 to 8 s, and the pilot gain K_p. The T_p/K_p-combinations were limited by the stability bounds that result from the motion of the closed loop zeros when changing K_p. Both low-limit as well as high-limit constraints were found for the pilot gain K_p.

Figure 6 shows the 189 combinations of prediction time T_p that were used in each of the eight tracks in the offline simulations. An additional handling requirement was also set, limiting the aircraft roll angle to 20 deg and roll rate to 10 deg/s. The markers represent the handling requirement test results. The stability range is shown by the continuous lines $K_{p_{\min}}$ and $K_{p_{\max}}$.

Results showed that, for each prediction time T_p, there exists a wide range of pilot gains that yield satisfactory trajectory-following performance. Selecting a small prediction time resulted in reduced path-following errors, but also led to considerable control effort. Conversely, a higher prediction time resulted in a reduced tracking performance with lower control effort. A good compromise for the prediction time was found to be 4 s [16].

The selected prediction time of 4 s proved to be too large, however, for the higher-bandwidth vertical aircraft dynamics, and resulted in an underdamped response. This is a common finding in the literature, and is generally resolved by reducing the effect of the aircraft vertical acceleration on the predicted vertical trajectory with a gain [11,13,17]. For the dynamics of the Cessna Citation 500, a gain of 0.5 proved satisfactory.

C. Visual and Haptic Display Scaling

The flight director control law used in this study, based on the circular-path flight-path prediction, results in the predicted aircraft position errors (lateral, vertical) relative to the path. The task of the pilot becomes simply to minimize these errors, involving a compensatory display that is either visual or haptic. For both the visual and haptic flight director displays, the predicted position errors are scaled by dividing it by the look-ahead distance of the prediction, $V_{\text{TAS}}T_p$, and multiplying it with a gain. To remove high-frequency oscillations that result from flying through turbulence, the flight director command signals were low-pass filtered with a first order filter with break frequency 6.67 rad/s (lag time constant 0.15 s).

IV. Experiment

An experiment was conducted to investigate pilot performance, workload, and attention-sharing effectiveness with the haptic flight director as compared with the visual flight director. The experimental procedure and setup are described next; the following section discusses the results.

A. Method

1. *Apparatus*

The experiment was conducted in a fixed-base, part-task flight simulator (Fig. 7). The flight deck consisted of two 17 in displays. The first display, (A) in Fig. 7, was positioned in front of the pilot and showed the basic flight instruments, including an airspeed indicator (V_{TAS}), primary flight display with flight director command bars, altimeter, navigation display, and instantaneous vertical speed indicator. The second display, (C), was used for the secondary task, discussed in Sec. IV.A.3, which is controlled using the numeric keypad, (D), attached to the pilot's left leg. A 2-DOF (pitch, roll) electrohydraulic control stick, (B), was used for aircraft control. Its properties are summarized in Table 1 and have been discussed in Sec. II. Elevator trim adjustments could be made using the throttle lever panel, (E). The out-of-the-window visual display, (F), presented a 60 by 40 deg perspective of the scenery and was used to improve the sensation of flight.

2. *Subjects and Instructions to Subjects*

Four professional airline pilots and one flight simulator pilot, all males, participated in the experiment (Table 2).

Their primary task was to control the aircraft along a curved approach trajectory as accurately as possible. Each trajectory was different, but of equal difficulty. It was provided to pilots using a common paper approach chart, and was also displayed on the navigation display.

The secondary task, described next, was instructed to be conducted as well as possible, but it was emphasized that performance in the primary task should prevail at all times.

3. *Secondary Task*

The secondary task served two goals. First, it served as the means of distracting pilot's visual attention from the primary task, as it

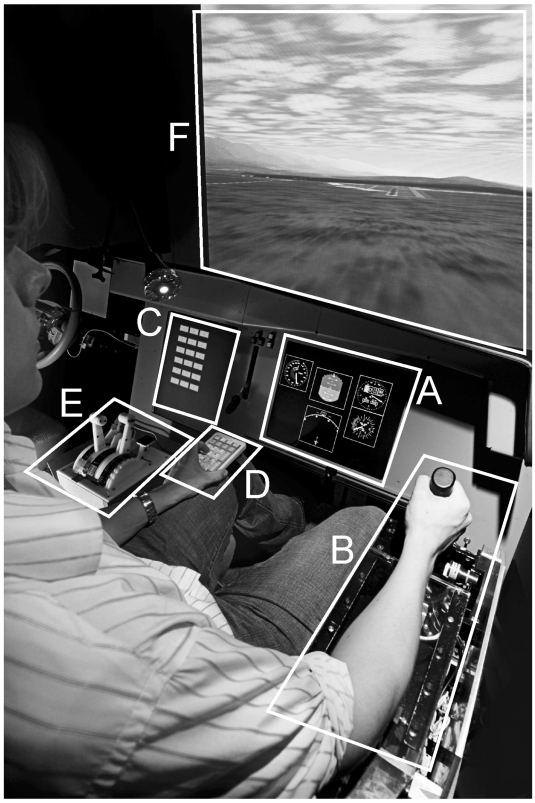

Fig. 7 Fixed-based, part-task experimental flight simulator.

forced pilots to temporarily look away from the primary flight display. Second, pilot performance in the secondary task performance can act as a measure for workload in the primary task [18].

The right choice of a secondary task is critical in ensuring its effectiveness as a workload measure, because it requires the pilot to work at "willing-to-spend capacity" throughout the experiment [18]. If this does not occur or, likewise, the length of the experiment results in considerable fatiguing of the pilot, results will not be conclusive. With this in mind, as means of redundancy, the subjective NASA task load index (TLX) rating scale was also used [19]. If the secondary task is successful, the TLX will show no or little sensitivity between conditions, because pilots are then indeed working at full capacity. If the secondary task fails, however, the TLX would, in theory, provide a usable workload measure.

The fixed-paced secondary task involved the identification and execution of an annunciator panel event. At random intervals, illumination of four out of 18 virtual push buttons (C in Fig. 7) occurred, accompanied by an auditory warning. Each of the four randomly illuminated buttons in the 3×6-array displayed a random number between one and nine. Two of these numbers were identical, and the pilot was required to push this key on the numeric keypad (D in Fig. 7).

The random intervals were selected from a skewed β-probability distribution, having a characteristic long toe, such that short interval times would be varied with occasional longer intervals, increasing

Table 2 Characteristics of the pilot subjects

Pilot	Age	Hours	Types of aircraft
A	29	1,200	Single-engine, Pa3/Pa43, Cessna Citation II
B	66	13,200	Single-engine, DC-3, DC-8, B747, Cessna Citation II
C	39	150	Flight simulator (B737)
D	30	4,400	F50, B737NG
E	39	5,200	Single-engine, Metro II, F50, Cessna Citation II, B767

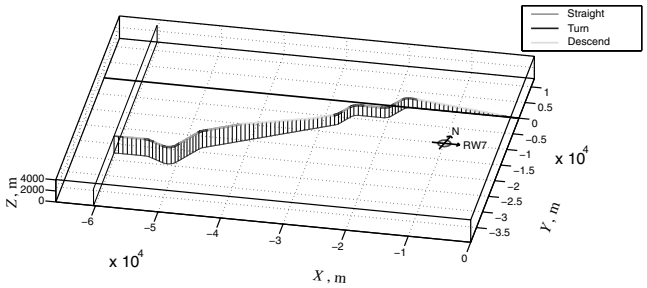

Fig. 8 Example approach track subdivided in 16 characteristic elements.

task complexity. Pilots were allowed to complete the task within 5 s after the auditory warning. Then, it timed out and a new event occurred after a new randomly selected interval. The time to complete each event was logged, as well as whether the answer was correct and the amount of events which could not be resolved in time.

Two levels of secondary task load, "Low" and "High," were defined by different interval times T_{int}. The interval time distributions were

$$\begin{aligned} T_{\text{int,LOW}} &= 7.5 + 7.5\beta(\alpha = 2, \beta = 3) \\ T_{\text{int,HIGH}} &= 2 + 5\beta(\alpha = 2, \beta = 3) \end{aligned} \tag{3}$$

For $T_{\text{int,LOW}}$, the mean was 10 s, the interval was [7.5, 15.0] s, and the standard deviation (STD) was 1.0 s. For $T_{\text{int,HIGH}}$, the mean was 4 s, the interval was [2.0, 7.0] s, and the STD was 1.5 s.

4. Approach Trajectory Geometry

The approaches in the experiment were towards Santa Barbara Municipal Airport, RW7. All (fictitious) approach trajectories consisted of an equal number of characteristic track elements occurring in the same order. Figure 8 shows one of the trajectories.

Each trajectory consisted of seven straight legs (SL), six horizontal rate-one (3 deg/s) turns (HT), one rate-one descending turn, and two 3-deg descents (DC). Trajectories started at 5000 ft and consisted of four straight legs with three turns in between, followed by a descent to 3000 ft, three turns with three straight legs in between, and were completed by a descending turn and the final descent.

The straight legs were selected from three different lengths: 1.5 n mile (2778 m), 2.0 n mile (3704 m), and 3.0 n mile (5556 m). The rate-one horizontal turns were selected from three different heading changes: ± 30, ± 60, and ± 90 deg. The two 3-deg descents involved altitude changes from 5000 to 3000 ft (1524 to 914 m) and from 3000 to 0 ft. The final turn was a 3-deg descending turn (60 deg) to the last descent, i.e., the glideslope.

A random generator produced six different tracks of approximately equal difficulty.

5. Independent Variables

Two independent variables were varied: 1) control type CT (three levels): visual flight director (VFD), haptic flight director without center cue (HFD1), and haptic flight director with center cue (HFD2); and 2) secondary task load STL (two levels): low and high as defined in Sec. IV.A.3.

6. Experimental Design and Procedure

A full-factorial within-subjects design was applied, yielding six conditions. The conditions were randomized over the experiment. Each pilot conducted various training sessions on a training approach trajectory, accustoming to the aircraft handling with the three control types and the secondary task. A minimum of three approaches (each of 15 min duration), one for each control type with varying secondary task load, were carried out during training, with the possibility to train more to attain confidence. None of the pilots required more than 1 h of training.

After training, all pilots performed six approaches in the six experimental conditions in random order and on random approach

Table 3 Characteristic values of the patchy turbulence field ($V_{TAS} = 75$ m/s and $L_g = 100$ m)

	u_g		v_g		w_g		$u_{g,\text{asymm}}$		$\alpha_{g,\text{asymm}}$	
	m/s	kn	m/s	kn	m/s	kn	m/s	kn	m/s	kn
min	0.4514	0.8774	0.8653	1.6820	0.8539	1.6598	0.6258	1.2165	0.7759	1.5083
max	−0.3886	−0.7554	−0.5776	−1.1227	−0.9746	−1.8945	−0.5777	−1.1229	−0.9328	−1.8132
σ	0.1193	0.2319	0.2196	0.4270	0.2304	0.4478	0.1488	0.2892	0.2207	0.4290

trajectories (no replications) serving as measurements. Each run lasted approximately 1000 s, with 10 s run-in time and 10 s run-out time. After each trial, pilots were asked to rate their workload using NASA-TLX. After completing all trials, a questionnaire allowed pilots to communicate their opinions on various aspects of the experiment.

7. *Aircraft Model*

The aircraft motion was simulated using a 6-DOF nonlinear model of the Cessna Citation 500 [20]. The aircraft was equipped with an engaged autothrottle, maintaining airspeed at 75 m/s (146 kn TAS). A yaw damper and turn-coordinator were active to improve lateral handling. The aircraft was controlled using aileron and elevator, of which the latter could be manually trimmed. No configuration changes (flaps, gear) were required.

8. *Atmospheric Turbulence Model*

A patchy turbulence field as described by Van de Moesdijk [21] was used. This model differs from the standard Dryden turbulence model [22] in that the turbulence consists of regions of higher energy alternated with relatively calm periods, more closely resembling actual turbulence.

Parameters for the generation of patchy turbulence were derived from Mulder et al. [23] using the same turbulence scale length, but reducing its magnitude to 25%, resulting in a light turbulence field. Table 3 shows characteristics of the five parameters describing the turbulence field: turbulence velocities in longitudinal u_g, lateral v_g, and vertical w_g directions; asymmetric gust velocities in horizontal $u_{g,\text{asymm}}$ and vertical $\alpha_{g,\text{asymm}}$ directions. The characteristic gust length L_g was set at 100 m, the Kurtosis parameter, describing the deviation from a Gaussian distribution was fixed at 4.5 and the patchiness parameter, controlling average patch length, was set at 0.7 [21].

9. *Dependent Measures*

Five types of performance variables acted as dependent measures: 1) control activity, defined as aileron δ_a and aileron rate $\dot{\delta}_a$ for lateral control and elevator δ_e and elevator rate $\dot{\delta}_e$ for vertical control; 2) aircraft attitude variations, i.e., roll angle ϕ and roll rate $\dot{\phi}$ for lateral attitude and pitch θ and pitch rate $\dot{\theta}$ for vertical attitude; 3) path-following performance, defined laterally as the track angle error χ_e and cross-track error x_e, and vertically with the flight-path angle error γ_e and vertical position error z_e; 4) secondary task performance, defined as the mean task execution time T_{task}, and its standard deviation; and 5) pilot subjective workload: the NASA-TLX scores.

Because the experiment trajectories involved descents and use was made of an ICAO standard atmosphere model in the simulation, trimmed elevator position as well as steady-state pitch angles differed at different altitudes. The values have therefore been normalized around the mean value at the specific altitude. Small consistent differences were removed by normalization around the mean, indicated by "Nrm." in the following.

B. Experiment Hypotheses

The first hypothesis was that the haptic flight director yields better path-following performance. The tactile modality has lower latencies as compared with the visual modality, and involving pilots in a tactile-motor task enables them to follow the flight director commands with a higher bandwidth.

The second hypothesis was that the haptic flight director results in lower pilot workload, because the primary task and the secondary task can be conducted using two modalities instead of only one. Dividing information over different modalities is expected to enable pilots to reduce their scanning effort.

The third hypothesis was that the higher secondary task load leads to a reduction of performance and higher workload for the visual flight director, but has no effect on these measures with the haptic flight director.

V. Results and Discussion

A. Subjective Data

1. *Workload Ratings*

The TLX workload ratings are shown in Fig. 9. Here, the mean ratings and weightings (left) show the individual contributions (subscales) of mental load, physical load, temporal load, effort, performance, and frustration levels to the total workload. The means and 95% confidence intervals for both absolute scores and normalized Z-scores are shown in the middle and right figures, respectively.

The ratings are lower for the haptic flight director as compared with the visual flight director, a highly significant effect on both the raw NASA-TLX scores ($F_{2,8} = 14.552$, $p < 0.01$) and the normalized Z-scores ($F_{2,8} = 192.328$, $p < 0.01$). This result supports hypothesis no. 2. Apparently, a better division of tasks over modalities resulted in a more efficient execution of multiple tasks, yielding lower pilot workload.

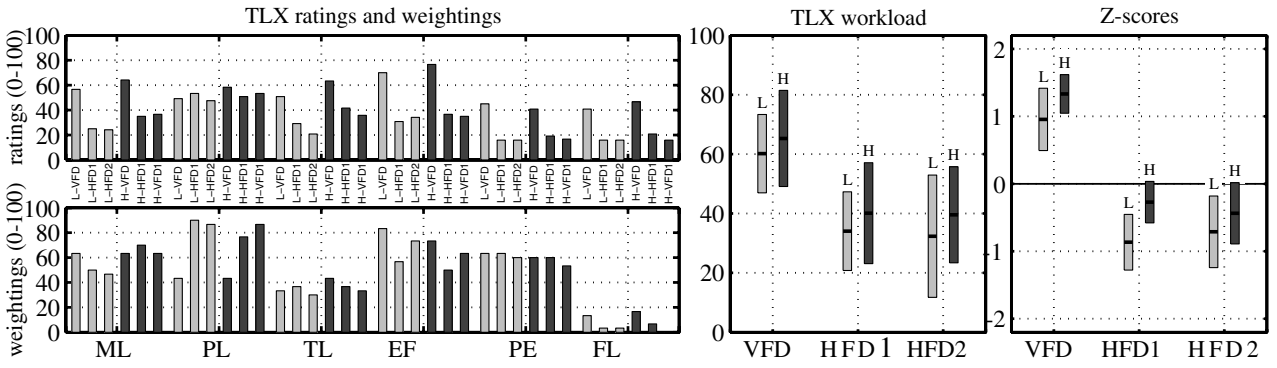

Fig. 9 TLX ratings for the three control modes and two secondary task loads.

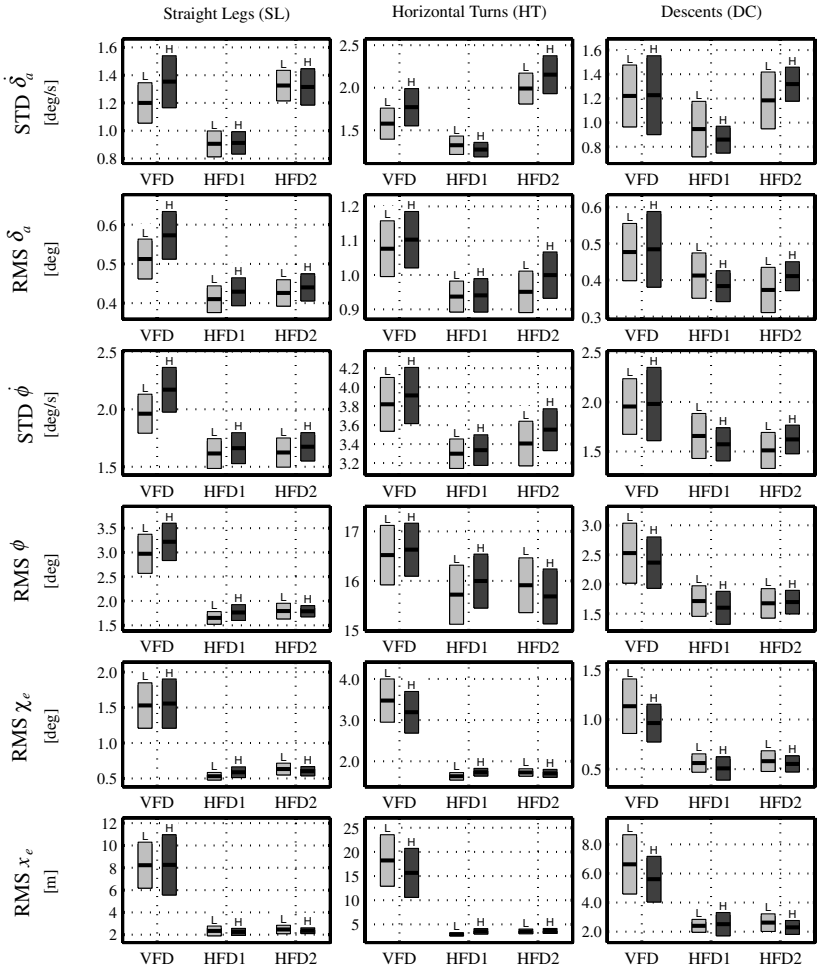

Fig. 10 Means and 95% confidence intervals of the lateral dependent measures (all subjects).

The average workload increased for the high secondary task load level as compared with the low load level, an effect that is only marginally significant, however, in the raw TLX scores ($F_{2,8} = 6.287,\ p = 0.066$) and not significant for the normalized Z-scores. The high load level required too little extra cognitive and/or attentional resources than the low load level.

The TLX subscale ratings indicate that the HFD leads to a reduction in all subscales, except the experienced physical load, which remained unaffected. In the subscale weightings, pilots indicated a relative increase of physical load with the haptic flight director as the most predominant contributor to the total workload. No differences were found between the HFD with and without the center cue, i.e., HFD2 and HFD1, respectively.

2. *Questionnaire*

In the questionnaire, three pilots indicated that the forces provided by the haptic flight director were good, whereas two pilots found them too high. On average, the forces required to control the aircraft were considered appropriate. All pilots agreed (of which four strongly) that the tactile cues were a useful source of information, and that the tactile cues allowed them to react more directly to the commands of the flight director. All agreed that the tactile cues increased their confidence to move their visual attention away from the primary flight display to conduct the secondary task.

The usefulness of the center cue in HFD2 was rated inconsistently: three pilots found it not very useful, two pilots found it a useful addition to the haptic flight director.

Overall, most pilots (two strongly agreed, one agreed, two were neutral) expressed their confidence in the haptic flight director as a support in tasks involving manually conducting complex approaches.

B. Primary Task Measures

The means and 95% confidence intervals of all dependent measures for the three characteristic trajectory elements (SL, HT, and DC) are shown in Figs. 10 and 11. In these figures, results are shown for the three control modes (VFD, HFD1, and HFD2) and for the low and high secondary task load levels. Furthermore, results are averaged for the three trajectory elements: straight legs (SL), rate-one horizontal turns (HT), and 3 deg descents (DC). Table 4 shows the results of a full-factorial analysis of variance (ANOVA).

Figures 10 and 11 clearly show an overall decrease in both the means as well as the standard deviations of practically all dependent measures for the haptic flight director as compared with the visual flight director. In the following, some of the results will be discussed in more detail.

1. *Path-Following Performance*

Lateral path-following performance in terms of lateral cross-track errors (x_e) improved considerably with the haptic flight director, a highly significant effect (ST: $F_{2,8} = 12.251,\ p < 0.01$; HT: $F_{2,8} = 10.933,\ p < 0.01$; DC: $F_{2,8} = 23.208,\ p < 0.01$). The same was found for the aircraft track angle errors χ_e (ST: $F_{2,8} = 16.901,\ p < 0.01$; HT: $F_{2,8} = 27.805,\ p < 0.01$; DC: $F_{2,8} = 19.022,\ p < 0.01$).

Vertical path-following performance improved significantly as well, both in terms of the vertical position error z_e (SL: $F_{2,8} = 6.034,\ p = 0.025$; HT: $F_{2,8} = 12.210,\ p < 0.01$; DC: $F_{2,8} = 7.260,\ p = 0.016$) as well as the flight-path angle error γ_e (SL: $F_{2,8} = 25.502,\ p < 0.01$; HT: $F_{2,8} = 90.036\ ,\ p < 0.01$; DC: $F_{2,8} = 13.910\ p < 0.01$).

Figures 10 and 11 further show that performance is much better in the straight and level segments of the trajectory as compared with the horizontal turns. The reduction in performance in these turns was

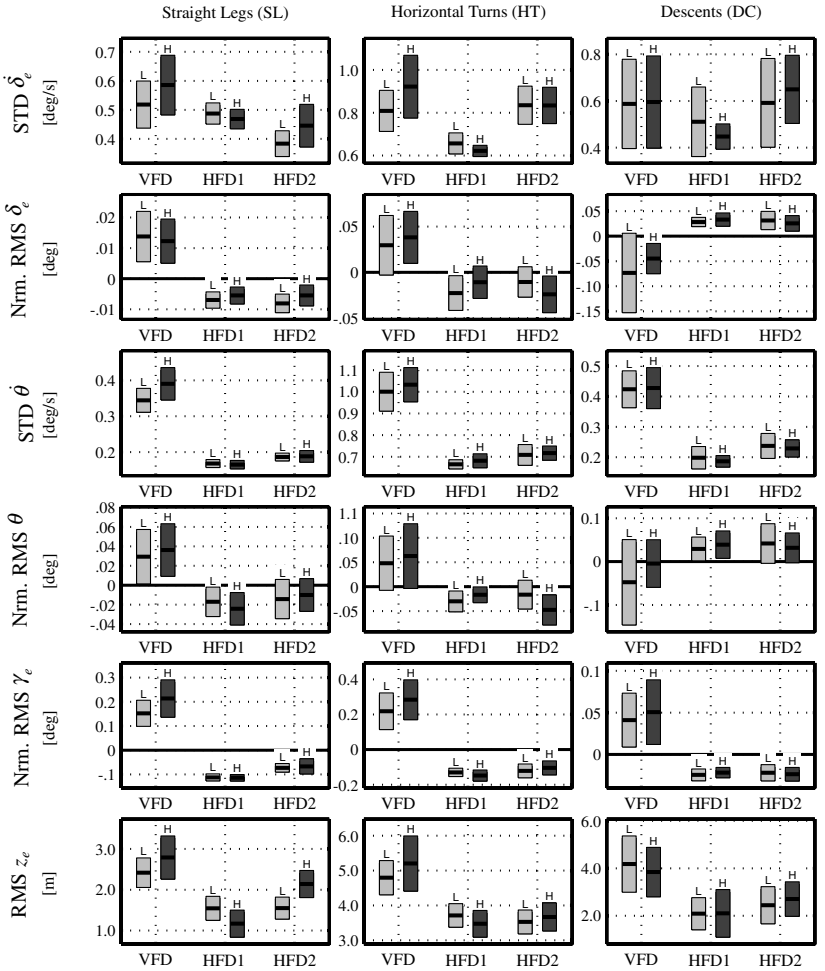

Fig. 11 Means and 95% confidence intervals of the vertical dependent measures (all subjects).

much stronger with the visual flight director as compared with the haptic flight director, with which performance reduced only slightly.

Summarizing, path-following performance greatly improves with the haptic flight director, supporting hypothesis no. 1. No differences were found between the HFD with and without the center cue. Surprisingly, no effects were found at all for the secondary task load level, not even for the visual flight director.

2. Aircraft Attitude Variations

Figures 10 and 11 clearly illustrate that the use of the haptic flight director results in a remarkable reduction of all dependent measures that relate to aircraft attitude variations. Roll angles ϕ (SL: $F_{2,8} = 21.882$, $p < 0.01$; HT: $F_{2,8} = 7.388$ $p = 0.015$; DC: $F_{2,8} = 13.279$, $p < 0.01$), roll rates $\dot{\phi}$ (SL: $F_{2,8} = 12.450$, $p < 0.01$; HT: $F_{2,8} = 17.095$, $p < 0.01$; DC: $F_{2,8} = 10.336$,

Table 4 Results of full-factorial ANOVA on lateral and vertical dependent measures[a]

Lateral	Control activity						Inner-loop measures						Path-following performance					
	$\dot{\delta}_a$			δ_a			$\dot{\phi}$			ϕ			χ_e			x_e		
Track element	SL	HT	DC	SL	HT	DC	SL	HT	DC	SL	HT	DC	SL	HT	DC	SL	HT	DC
Variable	*Main effects*																	
CT	⋆⋆	⋆⋆	⋆	⋆⋆	⋆⋆	⋆	⋆⋆	⋆⋆	⋆⋆	⋆⋆	⋆	⋆⋆	⋆⋆	⋆⋆	⋆⋆	⋆⋆	⋆⋆	⋆⋆
STL	·	·	·	○	·	·	○	·	·	·	·	·	·	·	·	·	·	·
Two-way interaction																		
CT × STL	·	·	·	·	·	·	·	·	·	·	·	·	·	·	·	·	·	·

Vertical	Control activity						Inner-loop measures						Path-following performance					
	$\dot{\delta}_e$			Nrm. δ_e			$\dot{\theta}$			Nrm. θ			Nrm. γ_e			z_e		
Track element	SL	HT	DC	SL	HT	DC	SL	HT	DC	SL	HT	DC	SL	HT	DC	SL	HT	DC
Variable	*Main effects*																	
CT	·	⋆	○	⋆⋆	⋆⋆	⋆⋆	⋆⋆	⋆⋆	⋆⋆	⋆⋆	⋆⋆	⋆⋆	⋆⋆	⋆⋆	⋆⋆	⋆	⋆⋆	⋆
STL	⋆	·	·	·	·	·	·	·	·	·	·	·	·	·	·	·	·	·
Two-way interaction																		
CT × STL	·	·	⋆⋆	·	·	·	·	·	·	·	·	·	·	·	·	·	⋆	·

[a]In this table, ⋆⋆ represents chance level $p \leq 0.01$, ⋆ chance level $0.01 \leq p \leq 0.05$, ○ chance level $0.05 \leq p \leq 0.10$, and · not significant.

$p < 0.01$), pitch angles θ (SL: $F_{2,8} = 18.869$, $p < 0.01$; HT: $F_{2,8} = 33.311$, $p < 0.01$; DC: $F_{2,8} = 17.953$, $p < 0.01$) as well as the pitch rates $\dot{\theta}$ (SL: $F_{2,8} = 45.506$, $p < 0.01$; HT: $F_{2,8} = 197.381$, $p < 0.01$; DC: $F_{2,8} = 49.171$, $p < 0.01$) all decrease significantly as compared with flying with the visual flight director.

Again, no differences were found between the two haptic flight director settings (HFD1 and HFD2), and again the secondary task load level had no significant effect at all.

3. Control Activity

The effect of the control type on pilot control activity depends on the trajectory segment considered. In both straight legs and horizontal turns the effect of the control type on control command rates ($\dot{\delta}_a$, $\dot{\delta}_e$), was more profound than in descents, generally yielding the smallest rates for HFD1. The effect of control type on control rates is weaker in vertical control ($\dot{\delta}_e$; SL: no significance; HT: $F_{2,8} = 4.628$, $p = 0.046$; DC: $F_{2,8} = 3.959$, $p = 0.064$) compared with lateral control ($\dot{\delta}_a$; SL: $F_{2,8} = 9.171$, $p < 0.01$; HT: $F_{2,8} = 17.148$, $p < 0.01$; DC: $F_{2,8} = 8.157$, $p = 0.012$). Commanded control angles in case of HFD1 and HFD2 are generally closer to the steady-state values and their spread is smaller, as compared with the visual flight director, resulting in a highly significant effect for elevator δ_e (SL: $F_{2,8} = 22.042$, $p < 0.01$; HT: $F_{2,8} = 23.525$, $p < 0.01$; DC: $F_{2,8} = 28.864$, $p < 0.01$) and aileron δ_a (SL: $F_{2,8} = 9.163$, $p < 0.01$; HT: $F_{2,8} = 16.931$, $p < 0.01$; DC: $F_{2,8} = 6.651$, $p = 0.020$).

4. Effects of the Secondary Task Load

As has been discussed in preceding sections, there were no statistically significant effects of the secondary task load on all of the dependent measures, except for the elevator rate, for which no direct explanation can be found. This is enough support to reject hypothesis no. 3.

C. Secondary Task Measures

Figure 12 shows the mean task execution time T_{task} (left) and the variation in this execution time (right), for the three control types and the two secondary task load levels.

The variability in task completion time decreased significantly for the haptic flight directors HFD1 and HFD2 as compared with the visual flight director (STD T_{task}; $F_{2,8} = 9.415$, $p < 0.01$). The mean secondary task execution time remained unaffected, however.

Apparently, in this experiment, increasing the secondary task load level did not have any significant effect on the primary task performance measures. Possible explanations are that the secondary task was too simple in both settings, that the change in difficulty level was too small, or that pilots had no problem dividing their attention.

D. Pilot Control in the Frequency Domain

Pilot control behavior can be investigated in the frequency domain through inspecting power spectral density (PSD) estimates of various control-related measures. Figure 13 depicts the mean PSD estimates for the three control types (VFD, HFD1, HFD2), averaged over all experimental data. PSDs are shown for commanded control angles (δ_a, δ_e), associated control moments (M_x, M_y), and stick positions (θ_x, θ_y), averaged over all subjects. As could have been expected from the discussion in the preceding section, secondary task load level did not result in any differences in the PSD estimates. Therefore, each line represents the mean of ten PSD estimates resulting from ten flights, conducted by the five pilots.

Lateral and vertical measures are shown on the left and right hand side, respectively. From top to bottom the figures show the magnitudes of aileron and elevator control deflections (δ_a, δ_e), the exerted stick moments (M_x, M_y), and control stick positions in roll and pitch (θ_x, θ_y), respectively.

A first observation is that the PSD magnitudes are generally much higher for the visual flight director as compared with the haptic flight director. The spread between pilots was also found to be much larger

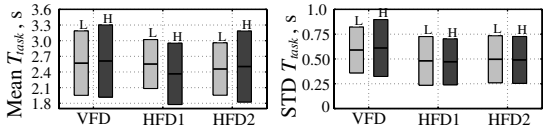

Fig. 12 Means and 95% confidence limits of secondary task execution time measures.

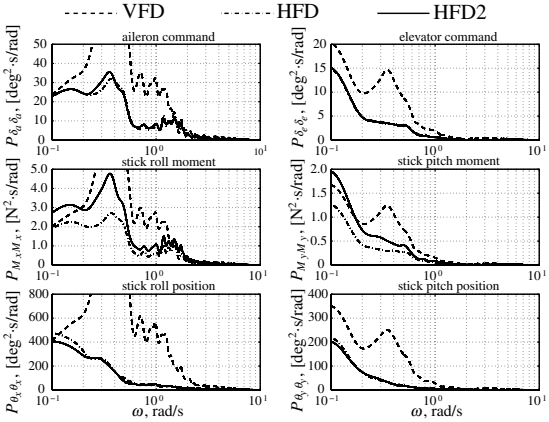

Fig. 13 PSDs of pilot control activity with VFD, HFD1, and HFD2 (all subjects).

for the visual flight director (not shown). This may indicate less-efficient control, more nonlinearities, and time-varying behavior, resulting in higher levels of pilot remnant with the visual flight director.

Exerted pilot moments (M_x and M_y), required in control with the haptic flight director with center cue, HFD2, are larger than those for HFD1, whereas the control commands (δ_a and δ_e) remain the same. This is as expected, because HFD2 requires pilots to overcome the center-cue breakout moment. As this is successfully compensated for in the control input relation, the PSD estimates of control stick positions are approximately equal for both haptic flight director settings.

The stick displacements (θ_x and θ_y) were much smaller for the haptic flight directors as compared with the visual FD, which is simply because of the completely different nature of the task. Whereas control stick excursions are required to perform a turn with the VFD, moving the stick off-center, in case of the haptic flight director a perturbing moment is compensated for, and pilots are only required to push the stick back towards the center.

In case of lateral control, both haptic flight directors HFD1 and HFD2 show two clear local maxima, reflecting an increase in control activity occurring between 0.3 and 0.4 rad/s and between 1.0 and 2.0 rad/s. This can be explained as follows. Essentially, the pilot is performing two control tasks in guiding the aircraft along the trajectory. First, the winding reference flight path requires pilots from time to time to initiate or end the turn, requiring control actions that are generally low-frequency and have a relatively large magnitude. These account for the maximum found between 0.3 and 0.4 rad/s.

The second type of control is related to the disturbance-rejection task, where pilots attempt to suppress the effects of turbulence. These control actions are generally high-frequency, have a smaller magnitude, and account for the maximum found between 1.0 and 2.0 rad/s.

Summarizing, the PSDs indicate that with the haptic flight director pilots have been able to, unconsciously, separate these control tasks into separated frequency bands. With the visual flight director this task separation can not be readily observed in the PSD estimates, indicating a less efficient division of control.

In case of vertical control, an oscillatory peak occurs around 0.35 rad/s for control with the visual flight director, a peak that cannot be found with both haptic flight directors.

E. Discussion

1. Path-Following Performance and Attitude Variations

The highly significant increase in primary task performance supports hypothesis no. 1, that the advantages of the faster tactile-motor loop result in more accurate path-following control and a much smoother ride. There are four main causes for the superiority in performance. First, the tactile modality has a higher resolution in perceiving the motion of the flight director bars, as compared with the visually perceived motions from the primary flight display, with its limited size and resolution. Second, whereas tactile information is continuous, the visually perceived information must be sampled. Third, another contributor to increased performance may be of mechanical or dynamic origin. The moments generated by the haptic flight director directly act on the pilot's hand/arm, the inertia of which immediately generate small reaction forces opposite to the haptic cues. These forces, although small in magnitude, yield immediate control initiation when the tactile flight director moves the stick relative to the pilot's hand. Fourth, pilot neuromuscular reflexes will generate reaction forces, even before the pilot engages in conscious control.

2. Workload

Workload levels drop significantly with the haptic flight director, supporting hypothesis no. 2. Pilot TLX ratings and weightings show that the haptic flight directors increased the relative importance of physical workload. This was supported by the questionnaire, where pilots reported that, on average, the magnitude of the tactile cues was slightly too high.

3. Secondary Task

The lack of a significant relationship between secondary task load and the dependent measures leads to a rejection of hypothesis no. 3. It suggests that pilots have enough cognitive and attentional capacity to perform both tasks, without affecting primary and secondary task performance. As this applied for both secondary task load levels, the difference in task load did not result in significant effects. This was also supported by the small effects in NASA-TLX workload.

A potential cause for this is the limited amount of resources required to solve and execute the secondary task. It can be considered a simple, rule-based task, that does not require many cognitive as well as attentional resources. In the questionnaire, however, pilots did report to have more problems in dividing their attention at the high level of the secondary task.

4. Pilot Comments

All pilots adapted to the haptic flight director quickly and reported that the task soon became very intuitive. Pilots found the tactile cues a useful information source, complementing the flight director information perceived visually in a pleasant way. Generally, the tactile information gave them more confidence in keeping the aircraft on the trajectory when they had to shift their attention towards the secondary task.

5. The Haptic Flight Director Center Cue

Student Newman–Keuls range tests ($\alpha = 0.05$) did not support the anticipated advantage of the stick-centered cue preventing control towards a bias error, as performance differences between the two tactile displays were not significant. This may be the result of the cooperation or integration of both visual and tactile information, where the visual flight director indicates the centered position by means of the position of the needles with respect to the aircraft symbol.

In the short time spans that attentional resources were directed away, not observing the visual centered cue from the flight instruments, this bias would not have had the time to grow significantly. The effect of the tactile centered cue would therefore potentially show advantages when visual attention for the visual flight director is directed away for longer periods.

Only in roll control rates did the Student Newman–Kuels range tests separate HFD1 from HFD2 for all characteristic track elements. An interaction with the centered-cue breakout force, with its nonsmooth behavior on the breakout edges, may be the reason for the increased rate changes with HFD2.

6. Limitations of this Research, Future Work

In this study, the task of conducting manual approaches has been simplified, reducing many of the normal tasks considerably. The primary advantage of manual control over a completely automatic approach remains that the pilot retains full situational awareness of the control actions, as the pilot performs them himself. This study clearly showed that the haptic flight director outperforms the conventional flight director. Performance with a fully-automated system has not been investigated.

Other limitations of this research include the assumption that the full aircraft state is available, whereas in reality, comprehensive filtering of various sources is required for state reconstruction. Moreover, potential biomechanical coupling effects that may result from inflight accelerations and vibrations on the pilot's use of tactile cues remain unknown.

Future work focuses on investigating these biomechanical couplings, exploring other tuning possibilities of the haptic flight director to reduce physical workload, and examining the potentially beneficial effects of quickening the haptic flight director control commands.

VI. Conclusions

The haptic flight director, providing fast and continuous tactile information for manual aircraft flight control, showed great potential. In a multitasking manual approach scenario, pilot workload decreased significantly and path-following performance was much more accurate as compared with a visual flight director. The haptic interface successfully retained pilots in full manual control of the aircraft, resulting in high pilot confidence, quick adaptation and a high experienced intuitiveness in its use.

References

[1] Moray, N., "The Role of Attention in the Detection of Errors and the Diagnosis of Failures in Man-Machine Systems. Human Detection and Diagnosis of System Failures," *Human Detection and Diagnosis of System Failures*, edited by J. Rasmussen and W. B. Rouse, Plenum, New York, 1981, pp. 185–199.

[2] Moray, N., "Monitoring Behavior and Supervisory Control," *Handbook of Perception and Human Performance*, Vol. 2, edited by K. R. Boff, L. Kaufman, and J. P. Thomas, Wiley, New York, 1986, pp. 40.1–40.51.

[3] Moray, N., and Rotenberg, I., "Fault Management in Process Control: Eye Movements and Action," *Ergonomics*, Vol. 32, No. 11, 1989, pp. 1319–1342.

[4] Carbonnell, J. F., Ward, J. L., and Senders, J. W., "A Queuing Model of Visual Sampling: Experimental Validation," *IEEE Transactions on Man-Machine Systems*, Vol. MMS-9, 1968, pp. 82–87.

[5] Tanaka, K., and Matsumoto, K., "A Hierarchical Model of Pilot's Procedural Behavior for Cockpit Workload Analysis," *Transactions of the Japan Society for Aeronautical and Space Sciences*, Vol. 28, No. 82, 1986, pp. 230–239.

[6] Sheridan, T. B., "Automation, Authority and Angst—Revisited," *Proceedings of the Human Factors Society—35th Annual Meeting*, Human Factors and Ergonomics Society, Santa Monica, CA, 1991, pp. 2–6.

[7] Wickens, C. D., *Engineering Psychology and Human Performance*, 2nd ed., HarperCollins, New York, 1992.

[8] Hosman, R. J. A. W., Benard, J. B., and Fourquet, H., "Active and Passive Side Stick Controllers in Manual Aircraft Control," *Proceedings of the IEEE Conference on Systems, Man and Cybernetics*, IEEE, Piscataway, NJ, 1990, pp. 527–529.

[9] Van Paassen, M. M., "Biophysics in Aircraft Control. A Model of the Neuromuscular System of the Pilot's Arm," Ph.D. Dissertation, Faculty of Aerospace Engineering, Delft Univ. of Technology, Delft, The

Netherlands, 1994.
[10] Klapp, S. T., "Doing Two Things at Once: The Role of Temporal Compatibility," *Memory and Cognition*, Vol. 7, 1979, pp. 375–381.
[11] Lam, T. M., Mulder, M., Van Paassen, M. M., and Mulder, J. A., "Comparison of Control and Display Augmentation for Perspective Flight-Path Displays," *Journal of Guidance, Control, and Dynamics*, Vol. 29, No. 3, 2006, pp. 564–578.
[12] McRuer, D. T., and Jex, H. R., "A Review of Quasi-Linear Pilot Models," *IEEE Transactions on Human Factors in Electronics*, Vol. HFE-8, No. 3, 1967, pp. 231–249.
[13] Grunwald, A. J., Robertson, J. B., and Hatfield, J. J., "Evaluation of a Computer-Generated Perspective Tunnel Display for Flight-Path Following," NASA Technical Paper TP-1736, 1980.
[14] Grunwald, A. J., "Tunnel Display for Four-Dimensional Fixed-Wing Aircraft Approaches," *Journal of Guidance and Control*, Vol. 7, No. 3, 1984, pp. 369–377.
[15] Sachs, G., "Perspective Predictor/Flight-Path Display with Minimum Pilot Compensation," *Journal of Guidance, Control, and Dynamics*, Vol. 23, No. 3, 2000, pp. 420–429.
[16] De Stigter, S., Mulder, M., and Van Paassen, M. M., "On the Equivalence between Flight Directors and Flight-Path Predictors in Aircraft Guidance," AIAA Paper 2005-5962, 2005.
[17] Borst, C., Mulder, M., Van Paassen, M. M., and Mulder, J. A., "Path-Oriented Control/Display Augmentation for Perspective Flight-Path Displays," *Journal of Guidance, Control, and Dynamics*, Vol. 29, No. 4, 2006, pp. 780–791.
[18] Stassen, H. G., Johannsen, G., and Moray, N., "Internal Representation, Internal Model, Human Performance and Mental Workload," *Automatica*, Vol. 26, No. 4, 1990, pp. 811–820.
[19] Hart, S. G., and Staveland, L. E., "Development of NASA-TLX (Task Load Index): Results of Empirical and Theoretical Research," *Human Mental Workload*, edited by P. A. Hancock and N. Meshkati, Elsevier Science Publishers North Holland, Amsterdam, 1988, pp. 139–183.
[20] Van der Linden, C. A. A. M., "DASMAT: the Delft University Aircraft Simulation Model and Analysis Tool," Delft Univ. of Technology, Faculty of Aerospace Engineering, Report LR-781, Delft, The Netherlands, April 1996.
[21] Van de Moesdijk, G. A. J., "The Description of Patchy Atmospheric Turbulence, Based on a Non-Gaussian Simulation Technique," Delft Univ. of Technology, Faculty of Aerospace Engineering, Report LR-192, Delft, The Netherlands, February 1975.
[22] Mulder, J. A., and van der Vaart, J. C., *Aircraft Responses to Atmospheric Turbulence*, Lecture Notes, Delft Univ. of Technology, Delft, The Netherlands, 2002.
[23] Mulder, M., Veldhuijzen, A. R., Van Paassen, M. M., and Mulder, J. A., "Integrating Fly-by-Wire Controls with Perspective Flight-Path Displays," *Journal of Guidance, Control, and Dynamics*, Vol. 28, No. 6, 2005, pp. 1263–1274.